

# Numerical Simulation of Transient Free Convection in a Rectangular Cavity Filled with Porous Material Using Finite Element Formulations

D Jyosthna<sup>1,2</sup>, Lokesh Kalapala<sup>3,\*</sup>

## Abstract

*In this study, the finite element method is used to quantitatively explore transient free convection in porous cavities in order to understand the flow characteristics and heat conduction processes in the square cavities. In comparison to an uniform temperature gradient, the left wall is swiftly heated and the right wall is allowed to cool to a specific temperature. The horizontal walls are insulated on both sides. Dimensionless representations of the energy, Darcy and continuity equations are solved numerically. Equilibrium state between fluid and solid phases in porous material with a low Reynolds number and porosity was used to generate the results. To solve the dimensionless basic equations, a numerical finite element technique is applied. To solve a set of governing equations, a spatial discretization of triangular components with quadratic elements of 6 nodes and an implicit temporal integration approach are implemented. It can be concluded that the finite element formulation can be successfully implemented to analyze flow and heat transfer characteristics in porous medium with a relatively less computational time and coarse grid.*

**Keywords:** Darcy law, continuity equations, porous medium, heat transfer, finite element method

## INTRODUCTION

To improve heat transfer and increase the efficiency of energy devices, researchers in the field of heat transfer are constantly looking for innovative solutions. Natural convection and internal heat generation in voids filled with porous material are two of the strategies adopted for improving the thermal performance of power systems. The phenomenon has gained a significant amount of attention over the last four decades due to its vast variety of technical and scientific applications, such as fluid flow in geothermal energy, insulation material, filtration, petrochemical reservoirs, nuclear reactors,

and so on. It is impossible to explicitly compare flow across porous material to flow via a pipe because it is a very complicated process. The study of fluids in porous materials has progressed through time based on experimental results or analytical methods. The distribution of holes of different shapes and sizes is random in naturally porous substances. Natural porous materials include silt, sand, stone, flat-bread, timber, and human lungs. It is important to understand that the overall thermal conductivity of porous material is intricately dependent on the geometry of the material [1, 2].

Note also that there is a difference in the calculation of the total conductivity for solid and fluid phase heat conduction in parallel and in

### \*Author for Correspondence

Lokesh Kalapala

<sup>1</sup>Research Scholar, Department of Mechanical Engineering, Koneru Lakshmaiah Education Foundation, Vaddeswaram, Andhra Pradesh, India

<sup>2</sup>Research Scholar, Department of Mechanical Engineering, Sri Venkateswara University, Tirupathi, Andhra Pradesh, India

<sup>3</sup>Assistant Professor, Department of Mechanical Engineering, Koneru Lakshmaiah Education Foundation, Vaddeswaram, Andhra Pradesh, India

Received Date: August 18, 2023

Accepted Date: September 11, 2023

Published Date: September 22, 2023

**Citation:** D Jyosthna, Lokesh Kalapala. Numerical Simulation of Transient Free Convection in a Rectangular Cavity Filled with Porous Material Using Finite Element Formulations. Journal of Polymer & Composites. 2023;

series. The Darcy modelling approach represents the most fundamental flow model for porous material. Permeability of porous materials is matrix-dependent and irrespective of the flowing fluid. Described as the functional cross-sectional area transverse to the flow direction and offers a gauge of the matrix's porosity [3].

This physical system's mathematical model is developed and regulated using differential equations with specific limitations. In order to accomplish this, Darcy's law is often employed as well as the fundamental laws of conservation of mass and momentum. The basic assumption is that the continuum model is used with porous matrices. Walled areas heated from the sides are the most representative of permeable scaffolds that function in a vertical position, as in building insulation, mechanical refrigerators, and cryogenics [1]. Several scholars have reviewed studies on heat transport in porous material in recent years [2–11]. Previously, researchers utilised the finite difference and finite volume approaches to estimate heat transport via porous material. Minimal work has been done on solving the equations using Finite Element Method [12–16]. Several research on flow and heat transfer across porous materials have already been conducted during the last two decades [17–21]. DNS is used to analyse the most recent breakthroughs in numerical modelling of heat exchange in porous materials for microscopic and macroscopic investigation of convective heat porous medium [22].

Anirudh et al. [23] using OpenFoam examined the influence of the Prandtl number on heat transfer in porous materials. Kakur et al. [24] put together a mathematical model to better comprehend heat transfer and unsaturated circulation in porous materials. Majumder et al. [25] demonstrated that reduced Darcy numbers are favoured to improve heat transfer coefficients at higher Reynolds and Grashof numbers. Bovand et al. [26] observed that decreasing the Darcy number boosts the drop in pressure.

The porous inserts of equivalent diameter within a tube improve convective heat transfer significantly, and the corresponding flow resistance increases to a reasonable extent, particularly in laminar flow. It demonstrates that core flow improvement is an effective way for increasing heat transfer [27]. Increasing heat transfer efficiencies can be accomplished at the tradeoff of an acceptable pressure drop by employing porous inserts. The Nusselt number increases essentially linearly with increasing Reynolds number based upon pore diameter [28, 29].

In a porous medium circle, natural convection has been studied by Prasad and Kulacki [30]. They discovered that the localized rate of heat transmission is significantly higher close to the cold wall's top edge. In a longitudinal circle packed with densely saturated porous media, Prasad et al. [31] experimental studies of natural convection. The impact of radiation and viscous dissipation in a circular porous media has been studied by Badruddin et al. [32].

Due to the adaptability of the FEM in modelling layered structures and capacity to produce a complete field numerical solution, the finite element method technique (FEM) is used to examine the numerical solution of the issue [33–35]. In order to use the finite element, difference, and volume techniques, each partial differential equation must be transformed into an alternative collection of algebraic equations, the degree of which relies on how many elements are divided up into the physical domain. As a result, the number of algebraic equations formed increases as the quantity of partial differential equations implicated in an event increases. In general, it may be claimed that the quantity involved in an event is a multiple of the quantity of partial differential equations implicated. The benefits include significantly improved accuracy characteristics that allow integrating with bigger time steps and, generally, a more efficient resolution of nonlinear and linear challenges. For structural studies and fluid-structure interactions, the technique is currently frequently employed [36].

A simple mathematical formula known as Darcy's Law is a concise summary of many well-known facts. If there is no pressure drop over some distance, there is no flow. This is known as the

hydrostatic condition. In a pressure gradient, flow from high pressure to low pressure flows in the opposite direction of the increasing gradient. This is why Darcy's law has a negative sign. The higher the pressure gradient across a particular formation material, the higher the release rate. However, fluid release rates often change as the fluid flows through different formation materials. Proposed properties of porous material include homogeneity, thermal isotropy and saturation with fluids that are in local thermodynamic equilibrium with the solid matrix. Laminar and incompressible fluid flow. Both pressure work and viscous dissipation are considered insignificant. High-permeability housings produce high-flow circulation, and low-permeability housings produce low-flow circulation. Conduction is the dominant method of heat transfer at low Darcy numbers. The buoyancy increases as the number of darcy number increases. As a result, isothermal contours are more distorted for higher Darcy numbers, but match the shape of the case for lower Darcy numbers. The current study investigates the mechanics of fluid and heat flow in a rectangular cavity packed with porous materials by employing Darcy's formula and the momentum and energy equations. According to the findings of the preceding research, convective heat transfer with heat generation in rectangular cavities filled with uniform and porous materials and fluids has not yet found a workable solution. As a consequence, this study is absolutely unique, and the researchers hope that it will pique the curiosity of other experts in the subject.

## METHODOLOGY

### Theoretical Analysis and Model Description

Considering Figure 1 of a two-dimensional rectangular cavity proposed by Saeid et al. [37]. Assume the left vertical side of the cavity is instantly heated to a specific temperature  $T_h$  and the right vertical wall is instantly cooled to a specific temperature  $T_c$ , and the lateral walls are adiabatic. The flow in this research is considered to be in-compressible, steady state, Newtonian, and laminar. All characteristics except density are considered constant and the viscosity and energy factors are neglected.

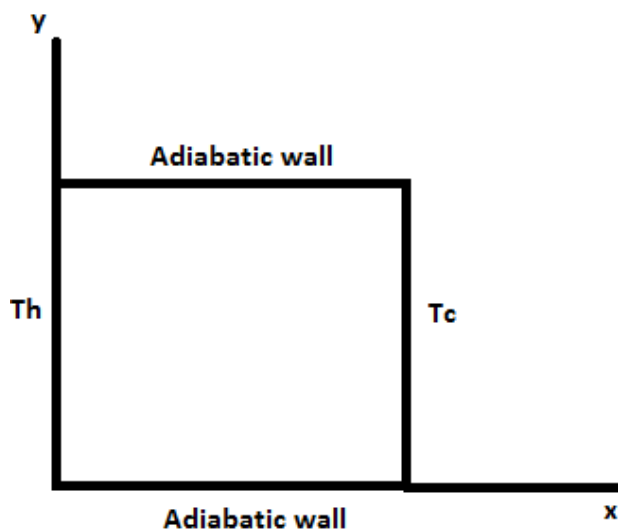


**Figure 1.** Diagram of an physical model indicating the adiabatic wall, the temperature difference in the vertical walls and the coordinate System.

### Governing Equations

Darcy's law, a constitutive equation that characterises fluid flow across porous material, is derived from phenomenology. Based on the findings of experiments on the flow of water through sand beds, Henry Darcy passed laws. The explanation for fluid permeability in hydrogeology and other earth sciences is also given. Through his investigations, Darcy established the conservation of momentum formula, but it wasn't until later that the Navier-Stokes equations were homogenised to get Darcy's law. The pressure differential that occurs when a fluid passes through a porous material diminishes as

the porosity parameter rises. As a result, the fluid's mass is decreased, which lowers both the fluid's and the dust particles' velocity. The temperature and velocity are raised by the Dufour parameter, but the concentration profile is barely altered. The velocity increases as the buoyancy parameter is increased. The medium is linearly stratified at constant wall temperature and concentration in the vertical plane with regard to the thermal conditions there. It is well known that lowering the keywall temperature of the cold wall requires increasing either the radiance parameter or the porosity parameter. Darcy's formulation is applicable to porous materials, and the fluid is considered to be a standard Boussinesq fluid. It appears logical to omit the viscous drag and inertia parts of the governing equations for low Darcy numbers and low particle Reynolds numbers. Equations 1, 2, and 3 respectively give the continuity equation, Darcy formulation, and the energy equations for an unsteady 2D flow in an isotropic and homogeneous porous material.

$$\frac{\partial u}{\partial x} + \frac{\partial v}{\partial y} = 0 \tag{1}$$

$$\frac{\partial u}{\partial y} - \frac{\partial v}{\partial x} = -\frac{g\beta K}{v} \frac{\partial T}{\partial x} \tag{2}$$

$$\sigma \frac{\partial T}{\partial t} + u \frac{\partial T}{\partial x} + v \frac{\partial T}{\partial y} = \alpha \left( \frac{\partial^2 T}{\partial x^2} + \frac{\partial^2 T}{\partial y^2} \right) \tag{3}$$

where u, v denoted are the two components of velocity along the x and the y axes and T is denoted as the working fluid's temperature. For the aforementioned equations, the beginning and boundary conditions are

Boundary conditions for the square cavity are given below.

$$u(x, y, 0) = v(x, y, 0) = 0, T(x, y, 0) = T_0 \tag{4}$$

$$u(0, y, t) = v(0, y, t) = 0, T(0, y, t) = T_h \tag{5}$$

$$u(L, y, t) = v(L, y, t) = 0, T(L, y, t) = T_c \tag{6}$$

$$u(x, 0, t) = v(x, 0, t) = 0, \partial T(x, 0, t)/\partial y = 0 \tag{7}$$

$$u(x, L, t) = v(x, L, t) = 0, \partial T(x, L, t)/\partial y = 0 \tag{8}$$

The given formula derives the dimensional version of the governing equations for an isotropic homogeneous porous material with stable layered architecture as  $T_o = (T_h + T_c)/2$ . Said et al. [37] defined the aforementioned formulation, the Nusselt number, and the average Nusselt number as physical quantities of interest.

$$\frac{\partial^2 \Psi}{\partial X^2} + \frac{\partial^2 \Psi}{\partial Y^2} = -Ra \frac{\partial \theta}{\partial X} \tag{9}$$

$$\frac{\partial \theta}{\partial \tau} + \frac{\partial \Psi}{\partial Y} \frac{\partial \theta}{\partial X} - \frac{\partial \Psi}{\partial X} \frac{\partial \theta}{\partial Y} = \frac{\partial^2 \theta}{\partial X^2} + \frac{\partial^2 \theta}{\partial Y^2} \tag{10}$$

$$\Psi(X, Y, 0) = 0, \theta(x, y, 0) = 0 \tag{11}$$

$$\Psi(0, Y, \tau) = 0, \theta(0, Y, \tau) = 0.5 \tag{12}$$

$$\Psi(1, Y, \tau) = 0, \theta(1, Y, \tau) = -0.5 \tag{13}$$

$$\Psi(X, 0, \tau) = 0, \partial \theta(X, 0, \tau)/\partial Y = 0 \tag{14}$$

$$\Psi(X, 1, \tau) = 0, \partial \theta(X, 1, \tau)/\partial Y = 0 \tag{15}$$

### Method of Solution

The finite element approach is used to numerically solve the governing equations for two-dimensional transient free convection. You can decide whether to describe the governing equations for the reference configuration or the present (or spatially deformed) configuration in a finite element analysis of deformation. As a result, operations like gradient (grad) and divergence (div) should only be used in one of the two configurations. An operator often uses a letter to designate the current

configuration. Otherwise, the six nodal components (square elements) are often capitalised when they are employed in the spatial composition in order to discretize space. The equations given above and boundary conditions with an implicit time integration technique were utilised to achieve the solution. The element stiffness matrix must be converted into a global system of equations in this stage, which calls for a transformation matrix. The pressure at the corner nodes and the velocity components in both mutually orthogonal directions are both contained in the global stiffness matrix. The second portion of the stiffness matrix contains the velocity component. The Jacobian matrix's element solution vector and determinant are calculated.

$$\frac{d^2\Psi}{dX^2} + \frac{\partial^2\Psi}{\partial Y^2} + Ra \cdot \frac{d\theta}{dX} = \sigma \quad (16)$$

$$\frac{d\theta}{d\tau} + \frac{d\Psi}{dY} \cdot \frac{d\theta}{dX} - \frac{d\Psi}{dX} \cdot \frac{d\theta}{dY} - \frac{d^2\theta}{dX^2} - \frac{d^2\theta}{dY^2} = \sigma \quad (17)$$

$$\int \left( \text{div}(\text{grad}\Psi) + Ra \cdot \frac{d\theta}{dX} \right) \delta\theta dV \quad (18)$$

$$= \int \left[ -\text{div}(\text{grad}\Psi \cdot \delta\theta) + \text{grad}\delta\Psi \text{grad}\Psi + Ra \cdot \frac{d\theta}{dX} \cdot \delta\theta \right] dV \quad (19)$$

$$= \int \left[ -\text{grad}\Psi \text{grad}(\delta\Psi) + Ra \cdot \frac{\partial\theta}{\partial X} \cdot d\theta \right] dV - \int \text{grad}(\Psi) \cdot \partial\theta \cdot a \cdot d\theta \quad (20)$$

$$\int \text{grad}(\Psi) \cdot \partial\theta \cdot a \cdot d\theta = \sigma \quad (21)$$

$$\int \left[ -\text{grad}(\Psi_{i+1}) \cdot \text{grad}(\delta\Psi) + Ra \cdot \frac{\partial\theta}{\partial X} \cdot \delta\theta \right] dV = \sigma \quad (22)$$

$$\int \left[ -\text{grad}(\Psi_{i+1})|_j \cdot \text{grad}(\delta\Psi) + Ra \cdot \frac{\partial\theta_{i+1}}{\partial X}|_j \cdot \delta\theta \right] dV = \sigma \quad (23)$$

$$\int \left[ -\text{grad}\Delta\Psi_{i+1}|_j \cdot \text{grad}\delta\Psi + Ra \cdot \frac{\partial\Delta\theta_{i+1}}{\partial X}|_j \cdot \delta\theta \right] dV = \sigma \quad (24)$$

Deriving further we get,

$$\frac{\delta\theta}{\partial\tau} + \frac{\partial\Psi}{dY} \cdot \frac{\partial\theta}{dX} - \frac{\partial\Psi}{dX} \cdot \frac{\partial\theta}{dY} - \frac{\partial^2\theta}{dX^2} - \frac{\partial^2\theta}{dY^2} = \sigma \quad (25)$$

$$\theta_{i+1} = \theta_i + h \left( [1 - \eta] \frac{\partial\theta_{i+1}}{\partial\tau} + \eta \cdot \frac{\partial\theta_i}{\partial\tau} \right) \quad (26)$$

$$\sigma = \theta_i + h \cdot \eta \left( \frac{\partial\theta - i}{\partial\tau} \right) + h(1 - \eta) \left( \frac{\partial\theta_{i+1}}{\partial\tau} \right) - \theta_{i+1} \quad (27)$$

$$= \int \theta_i \cdot \delta\theta + \left[ h \cdot \eta \frac{-d\Psi_i}{dY} \cdot \frac{d\theta_i}{dX} \cdot \delta\theta + \frac{\partial\Psi_i}{dX} \cdot \frac{\partial\theta_i}{dY} \cdot \delta\theta + \text{div}(\text{grad}\theta_i) \right] \cdot \delta\theta \dots$$

$$\dots - \theta_{i+1}^j \cdot \delta\theta + h(1 - \eta) \left[ \frac{-d\Psi_{i+1}^j}{dY} \cdot \frac{\partial\theta_{i+1}^j}{dX} \cdot \partial\theta \frac{\delta\Psi_{i+1}^j}{dX} \cdot \frac{d\theta_{i+1}^j}{dY} \delta\theta + \text{div}(\text{grad}\theta_{i+1}^j) \delta\theta \right] \dots$$

$$\dots - \Delta\theta_{i+1} \delta\theta + h(1 - \eta) \left[ \left( \frac{-\delta\Delta\Psi_{i+1}}{\partial Y} \cdot \frac{d\theta_{i+1}^j}{dX} - \frac{d\Psi_{i+1}}{dY} \cdot \frac{\partial\Delta\theta_{i+1}}{\partial X} + \frac{\partial\Delta\Psi_{i+1}}{\partial X} \cdot \frac{\partial\theta_{i+1}^j}{\partial Y} \dots \right) \right]$$

$$\dots + \frac{\partial\Psi_{i+1}^j}{dX} \cdot \frac{\partial\Delta\theta_{i+1}}{dY} \cdot d\theta + \text{div} \left( \text{grad}(\theta_{i+1}^j) \right) \delta\theta_{i+1} dV \quad (28)$$

$$\int \left[ \theta_i \delta\theta + h\eta \left( -\frac{d\Psi_i}{dY} \cdot \frac{d\theta}{dX} \delta\theta + \frac{d\Psi}{dX} \cdot \frac{d\theta}{dY} \delta\theta - \text{grad}\theta_i \cdot \text{grad}\delta\theta \right) \dots \right]$$

$$\dots - \theta_{i+1}^j \cdot \delta\theta + h(1 - \eta) \left[ -\frac{\delta\Psi_{i+1}^j}{dY} \cdot \frac{d\theta_{i+1}^j}{dX} \cdot \delta\theta + \frac{\delta\Psi_{i+1}^j}{dX} \cdot \frac{\partial\theta_{i+1}^j}{dY} \delta\theta - \text{grad}\theta_{i+1}^j \cdot \text{grad}\delta\theta \right] \dots \quad (29)$$

$$- \Delta\theta_{i+1} \cdot \delta\theta + h(1 - \eta) \left[ \left( -\frac{\partial\Delta\Psi_{i+1}}{dY} \cdot \frac{d\theta_{i+1}^j}{dX} - \frac{d\Psi_{i+1}}{dY} \cdot \frac{d\Delta\theta_{i+1}}{dX} + \frac{\partial\Delta\Psi_{i+1}}{dX} \cdot \frac{\delta\theta_{i+1}^j}{dY} \dots \right) \right]$$

$$\frac{\delta\Psi_{i+1}^j}{dX} + \frac{\delta\Delta\theta_{i+1}}{dY} \cdot \delta\theta - \text{grad}(\Delta\theta_{i+1}) \cdot \text{grad}\delta\theta dV \quad (30)$$

**Implementation**

Finite element method was used for the spatial discretization, 6 noded tet elements (quadratic elements) were used. Equations derived above along with boundary conditions along with an implicit scheme for the time integration were used. Figure 2 shows a schematic flow chart of the implementation of the solution.

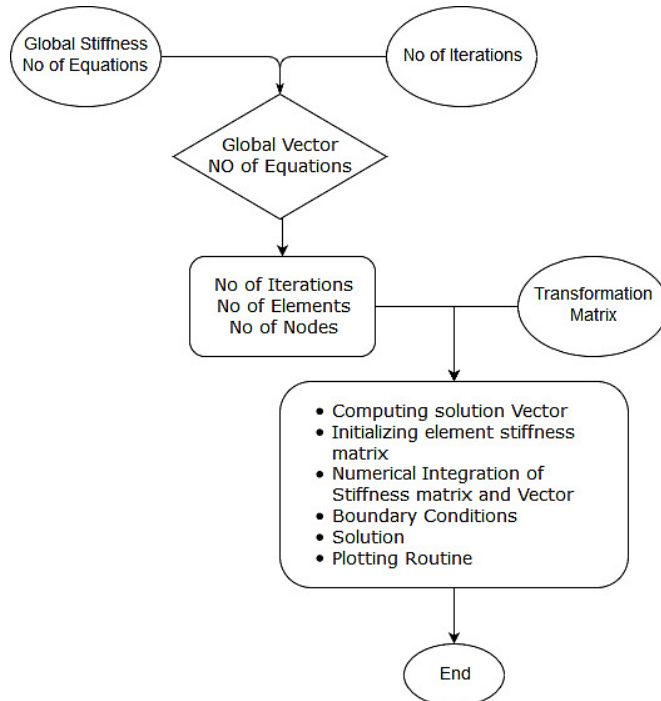
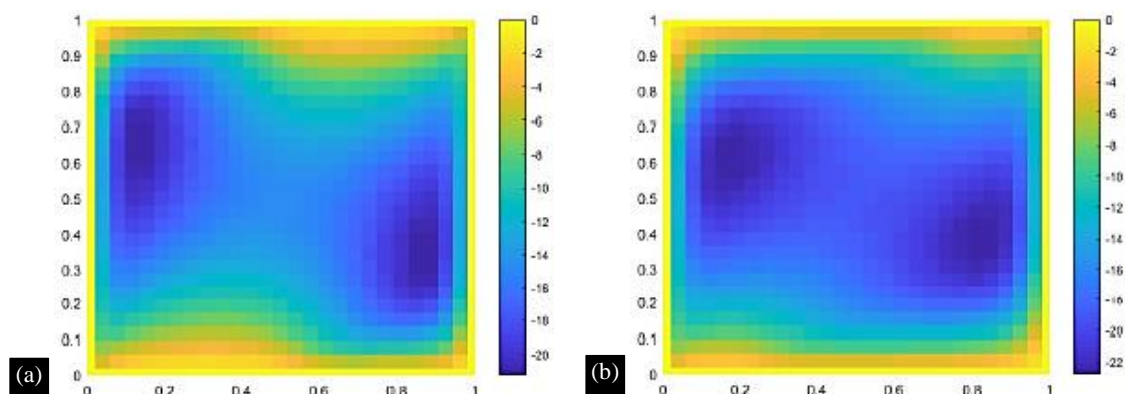


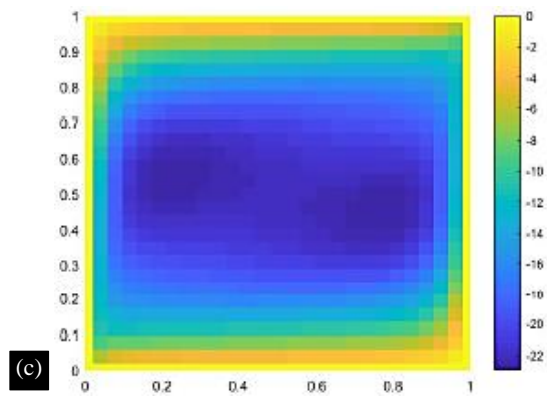
**Figure 2.** Flow Chart of the solution implementation.

During this step the transformation matrix is needed to transfer the element stiffness matrix into the global equation system. The global stiffness matrix contains the velocity components in both direction orthogonal to each other and then the pressure of the corner nodes. The velocity components are stored in the first and second section of the stiffness matrix. The solution vector for the element and the determinant of the Jacobian matrix is computed. The detail of the implementation of the algorithm is depicted in the flowchart shown.

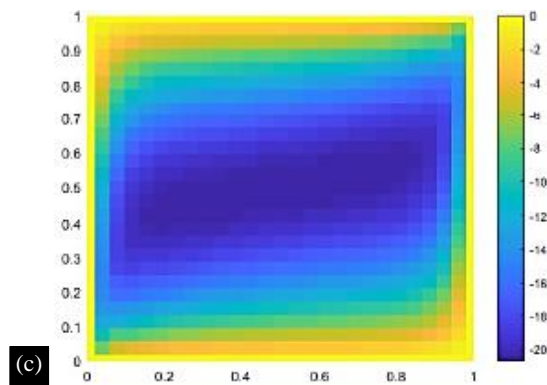
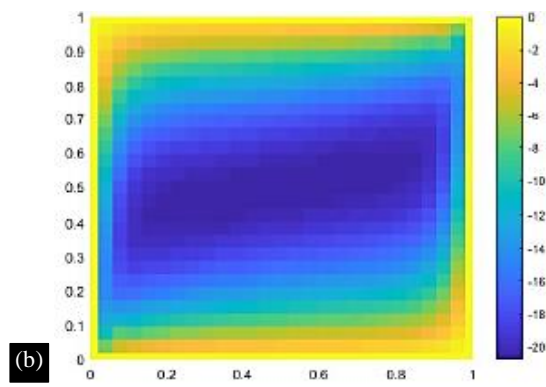
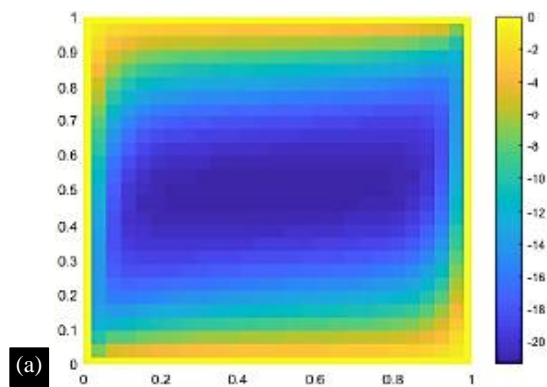
**RESULTS AND DISCUSSION**

A rectangular porous cavity’s streamlines (Figures 3 and 4) and isotherms of heat transfer caused by fluid flow are shown at different time steps from the first transient to the end steady state while boundary conditions are shown in Figure 5 and 6.

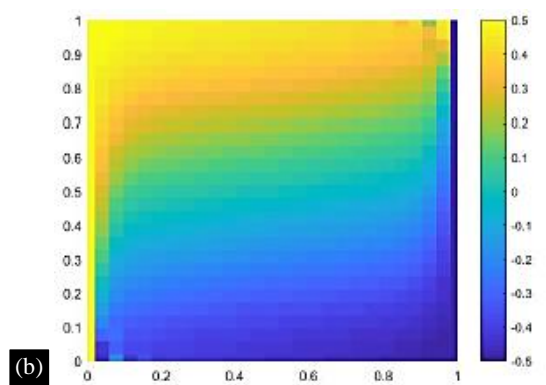
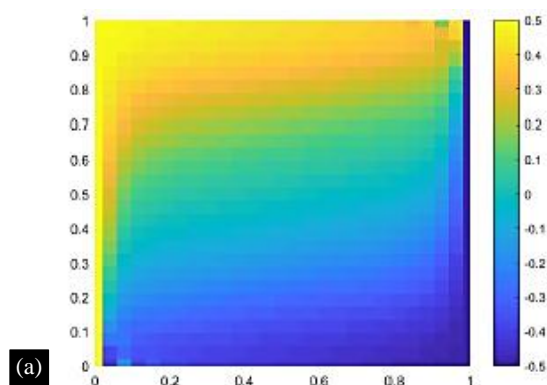




**Figure 3.** Streamlines for  $Ra = 1000$  (a) Streamlines for  $Ra = 1000$  and  $S = 0.0025$ , (b) Streamlines for  $Ra = 1000$  and  $S = 0.005$ , (c) Streamlines for  $Ra = 1000$  and  $S = 0.01$ .



**Figure 4.** Streamlines for  $Ra = 1000$  (a) Streamlines for  $Ra = 1000$  and  $S = 0.02$ , (b) Streamlines for  $Ra = 1000$  and  $S = 0.04$ , (c) Streamlines for  $Ra = 1000$  and  $S = 0.08$ .



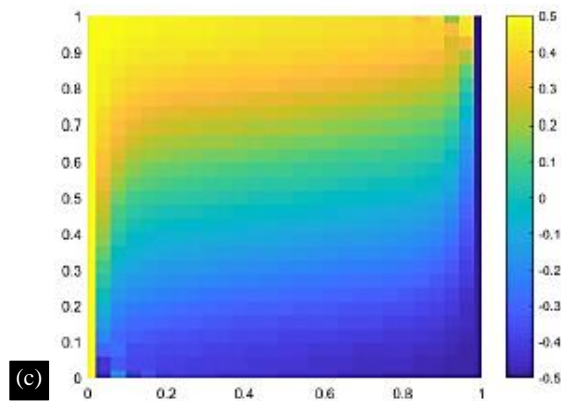


**Figure 5.** Isotherms for  $Ra = 1000$  (a) Isotherms for  $Ra = 1000$  and  $S = 0.02$ , (b) Isotherms for  $Ra = 1000$  and  $S = 0.04$ , (c) Isotherms for  $Ra = 1000$  and  $S = 0.08$ .

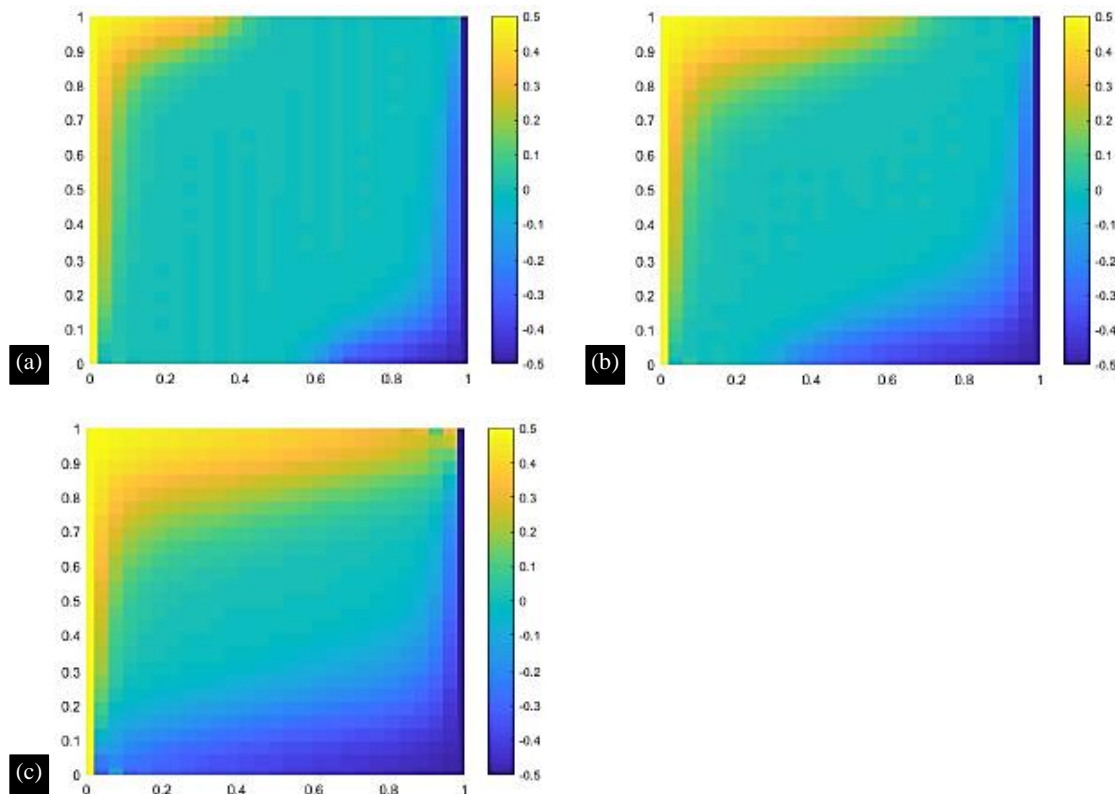


**Figure 6.** Isotherms for  $Ra = 1000$  (a) Isotherms for  $Ra = 1000$  and  $S = 0.0025$ , (b) Isotherms for  $Ra = 1000$  and  $S = 0.005$ , (c) Isotherm for  $Ra = 1000$  and  $S = 0.01$ .

Since the fluid is at rest during the initial stages of heat transfer, heat conduction is crucial to the process. As a result, the isotherm distribution is even and almost parallel to the cavity's walls where the fluid density is held. The fluid starts to rise and the flow starts to recirculate close to the hot wall. We can see that the flow circulation enlarges to fill the cavity's centre in the next time step. Convection starts to become significant in the heat transmission process at this point. Thermal and velocity boundary layers can also be seen. When the isotherms essentially parallelism, a conduction phenomenon happens. If the isotherm has a nearly symmetrical shape at low temperatures, the medium is homogeneous. The isotherms tend to remain parallel even when the thermal layers are thick. Isothermal pattern is significantly deformed in the cavity's centre and looks almost parallel to the cavity's insulated walls. Additionally, we are aware that low Rayleigh numbers produce steady state more slowly than high Rayleigh numbers, and vice versa.



## CONCLUSION

The objective of this study is to provide a FEM (finite element method) formulation and solution for inconsistent heat transfer across porous materials. It is shown how to solve for a rectangular cavity. The simulation results demonstrate that the solution found using the finite volume approach given by Saeid et al.[37] is in good agreement with the contours of streamlines and isotherms at various time steps of  $Ra = 1000$  by integrating the equations across the control volume via a fully implicit, unconditionally stable technique. Even with a coarse mesh and lower computational time and space similar results to the work by Saeid was achieved.

## REFERENCES

1. Nield D.A, Bejan. A, Convection in Porous Media, *Springer*, 2017.
2. Malviya C, Dwivedi A. K, Heat transfer in porous media: A review, *Journal of Industrial Pollution Control*.
3. Vadas P., Fluid Flow and Heat Transfer in Rotating Porous Media.
4. Abed R, Mohammed H. A, Munisamy K.M, Saeid N.H, Review of convection heat transfer and fluid flow in porous media with nanofluid, *Renewable and Sustainable Energy Reviews* 41 (2015) 715–734.
5. Kasaeian A, Daneshzarian R, Mahian O, Kolsi L, Chamkha A. J, Wongwises S, Pop I, Nanofluid flow and heat transfer in porous media: A review of the latest developments, *International Journal of Heat and Mass Transfer* 107 (2017) 778–791.
6. Misirlioglu A, The effect of rotating cylinder on the heat transfer in a square cavity filled with porous medium, *International journal of engineering science* 44 (18–19) (2006) 1173–1187.
7. Basak T, Roy S, Paul T, Pop I, Natural convection in a square cavity filled with a porous medium: effects of various thermal boundary conditions, *International Journal of Heat and Mass Transfer* 49 (7–8) (2006) 1430–1441.
8. Khanafer K, Vafai K, Effect of a circular cylinder and flexible wall on natural convective heat transfer characteristics in a cavity filled with a porous medium, *Applied Thermal Engineering* 181 (2020) 115989.
9. Nithiarasu P, Seetharamu K, Sundararajan T, Natural convective heat transfer in a fluid saturated variable porosity medium, *International Journal of Heat and Mass Transfer* 40 (16) (1997) 3955–3967.
10. Badruddin I. A, Al-Rashed A. A, Ahmed N. S, Kamangar S, Investigation of heat transfer in square porous-annulus, *International journal of heat and mass transfer* 55 (7–8) (2012) 2184–2192.
11. Abdulkadhim A, Abed A, Al-Farhany K, Computational investigation of conjugate heat transfer in cavity filled with saturated porous media, *Frontiers in Heat and Mass Transfer (FHMT)* 11.
12. Rajamani R, Srinivas C, Seetharamu K, Finite element analysis of convective heat transfer in porous media, *International journal for numerical methods in fluids* 11 (3) (1990) 331–339.
13. Soudagar M. E. M, Ahmed N. S, Badruddin I. A, et al., Fem formulation for heat and mass transfer in porous medium, in: *IOP conference series: materials science and engineering*, Vol. 225, IOP Publishing, 2017, p. 012022.
14. DIERSCII H, Primitive variable finite element solutions of free convection flows in porous media\*, *Akademie-Verlag Berlin* 61 (1981) 325.
15. Huang N, Szewczyk A, Li Y, Variational principles and finite element method for stress analysis of porous media, *International Journal for Numerical and Analytical Methods in Geomechanics* 14 (1) (1990) 1–26.
16. Khan T. Y, Baig M. A. A, Azeem, Ahamad N. A, Badruddin I. A, Heat and mass transfer with viscous dissipation in porous medium: Fem based methodology, in: *AIP Conference Proceedings*, Vol. 2104, AIP Publishing LLC, 2019, p. 030058.
17. Du H, Wang X, Forced convective heat transfer for fluid flowing through a porous medium with internal heat generation, *Heat Transfer Asian Research* 30 (3) (2001) 213–221. doi:10.1002/htj.1011.

18. Ganapathy R, Mohan A, Free convective darcy flow induced by a temperature gradient in a hemispherical porous medium, *Alexandria Engineering Journal* 57 (3) (2018) 2035–2042. doi:10.1016/j.aej.2017.05.015.
19. Mesgarpour M, Heydari A, Saedodin S, Numerical analysis of heat transfer and fluid flow in the bundle of porous tapered fins, *International Journal of Thermal Sciences* 135 (2019) 398–409.
20. Xua H.J, Xing Z.B, Wang F.Q, Cheng Z.M, Review on heat conduction, heat convection, thermal radiation and phase change heat transfer of nanofluids in porous media: *Fundamentals and applications*, *Chemical Engineering Science* 135 (2019) 462–483.
21. Ho J.Y, Leong K.C, Wong T.N, Experimental and numerical investigation of forced convection heat transfer in porous lattice structures produced by selective laser melting, *International Journal of Thermal Sciences* 137 (2019) 276–287.
22. Chu X, Yang G, Pandey S, Weigand B, Direct numerical simulation of convective heat transfer in porous media, *International Journal of Heat and Mass Transfer* 133 (2019) 11–20.
23. Anirudh K, Dhinakaran S, Effects of prandtl number on the forced convection heat transfer from a porous square cylinder, *International Journal of Heat and Mass Transfer* 126 (2018) 1358–1375.
24. Kacur J, Mihal P, Michal T<sup>3</sup>th, Numerical modeling of heat exchange and unsaturated–saturated flow in porous media, *Computers & Mathematics with Applications In Press, Corrected Proof* (2018).
25. Mojumder S, Saha S, Rahman M, Rahman M.M, Rabbi K. Md, Ibrahim T. A, Numerical study on mixed convection heat transfer in a porous l-shaped cavity, *Engineering Science and Technology, an International Journal* 20(1) (2017) 272–282.
26. Bovand M, Rashidi S, Esfahani J.A, Heat transfer enhancement and pressure drop penalty in porous solar heaters: Numerical simulations, *Solar Energy* 123 (2016) 145–159.
27. Huang Z, Nakayama A, Yang K, Yang C, Liu W, Enhancing heat transfer in the core flow by using porous medium insert in a tube, *International Journal of Heat and Mass Transfer* 53 (5–6) (2010) 1164–1174.
28. Pavel B. I, Mohamad A. A, An experimental and numerical study on heat transfer enhancement for gas heat exchangers fitted with porous media, *International Journal of Heat and Mass Transfer* 47 (23) (2004) 4939–4952.
29. Vafai K, Alkire R, Tien C, An experimental investigation of heat transfer in variable porosity media.
30. Prasad V, Kulacki F, Natural convection in a vertical porous annulus, *International journal of heat and mass transfer* 27 (2) (1984) 207–219.
31. Prasad V, Kulacki F, Kulkarni A, Free convection in a vertical, porous annulus with constant heat flux on the inner wall—experimental results, *International journal of heat and mass transfer* 29 (5) (1986) 713–723.
32. Badruddin I. A, Zainal Z, Khan Z. A, Mallick Z, Effect of viscous dissipation and radiation on natural convection in a porous medium embedded within vertical annulus, *International journal of thermal sciences* 46 (3) (2007) 221–227.
33. Zienkiewicz O, Taylor R, Nithiarasu P, The finite element method for fluid dynamics, vol. 6 (2015).
34. Reddy J. N, Introduction to the finite element method, *McGraw-Hill Education*, 2019.
35. Cook R. D, et al., Concepts and applications of finite element analysis, *John wiley & sons*, 2007.
36. Noh G, Bathe K.J, Further insights into an implicit time integration scheme for structural dynamics, *Computers & Structures* 202 (2018) 15–24.
37. Saeid N. H, Pop I, Transient free convection in a square cavity filled with a porous medium, *International Journal of Heat and Mass Transfer* 47 (2004) 1917–1924.